Jurnal Geologi dan Sumberdaya Mineral Vol. 26 No. 2 Mei 2025 hal. 113-127

Geo-Science

Jurnal Geologi dan Sumberdaya Mineral
Journal of Geology and Mineral Resources
Center for Geological Survey, Geological Agency, Ministry of Energy and Mineral Resources
Journal homepage: http://jgsm.geologi.esdm.go.id
ISSN 0853 - 9634, e-ISSN 2549 - 4759

# Characteristics of Ore-Bearing Vein in Banyuresmi, Cigudeg District, West Java Province: Constraints from Geological, Alteration, and Mineralization Aspects

## *Karakteristik Urat Bijih di Banyuresmi, Kecamatan Cigudeg, Provinsi Jawa Barat: Ditinjau dari Aspek Geologi, Alterasi, dan Mineralisasi*

**Ali Rifqi Alamudi, Mochamad Risyad Rizkyafdhal, Muhammad Bintang Firdaus, Dian Yesy Fatimah*, Dimas Setya Kusuma Wahjoedi**

Program Studi Teknik Geologi, Fakultas Teknologi Eksplorasi dan Produksi, Universitas Pertamina *email: dian.fatimah@universitaspertamina.ac.id

Submit: 9 June 2024, Revised: 20 May 2025, Approved: 31 May 2025, Online: 23 June 2025
DOI: 10.33332/jgsm.geologi.v26i2.902

**Abstract-** The study area of the ore-bearing vein system is located in Banyuresmi, Cigudeg District, ±13.6 km from the Gunung Pongkor deposits or ±45 km from Jakarta. The ore-bearing veins system is being operated by small-scale and traditional gold mines. Up to now, no peer-reviewed papers have been published on the geological conditions and ore characteristics in this area. This study aims to determine the distribution of lithology, geological structure, alteration zonation, and the mineralization characteristics of ore-bearing veins in the Banyuresmi area. To achieve the objectives, several research methods were employed, grouped into fieldwork (rock/vein sampling and geological structures measurement) and laboratory analysis (6 rock samples for petrography and 6 vein samples for ore microscopy). The results of this study indicate that the stratigraphy of the study area consists of porphyritic andesite units, which are overlain by lapilli tuff units and then followed by the formation of colluvial units. The geological structures that develop in the area of study, represented by normal faults, strike-slip faults, and thrust faults, are produced from the average value of maximum stress (σ1) for all tectonic phases, which have trend values of N32°E and N210°E (NE-SW). Hydrothermal alteration in the Banyuresmi vein system is divided into three zones: propylitic (chl-sm±ser±cb), argillic *(il±kao)*, and silicification *(qz)*. Mineralization in the area of study is dominated by ore minerals such as galena, sphalerite, pyrite, chalcopyrite, digenite, covellite, bornite, hematite, and pyrrhotite. These ore minerals are found in veins with quartz and quartz-clay composition, which consist of various textures including crustiform-colloform, massive,

***Abstrak-*** *Sistem urat pembawa bijih ini terletak ±13.6 km dari endapan Gunung Pongkor atau ±45 km dari Jakarta. Sistem urat pembawa bijih ini dioperasikan oleh tambang emas skala kecil dan tradisional. Hingga saat ini, belum ada publikasi makalah yang memuat kondisi geologi terkait karakteristik urat pembawa bijih di daerah tersebut. Studi ini bertujuan untuk mengetahui persebaran litologi, struktur geologi, dan zonasi alterasi, serta menentukan karakteristik mineralisasi dari urat pembawa bijih di daerah Banyuresmi. Untuk mencapai tujuan tersebut, digunakan beberapa metode penelitian yaitu pekerjaan lapangan (pengambilan sampel, dan pengukuran kedudukan struktur geologi) dan analisis laboratorium (analisis petrografi pada 6 sampel batuan serta analisis mineragrafi pada 6 sampel urat). Hasil dari penelitian ini menunjukkan bahwa stratigrafi daerah penelitian terdiri dari Satuan Andesit Porfiritik yang ditindih oleh Satuan Lapili Tuf dan kemudian disusul oleh terbentuknya Satuan Koluvial. Struktur geologi yang berkembang pada daerah penelitian berupa sesar normal, sesar geser, dan sesar naik dihasilkan dari harga rata-rata tegasan maksimum (σ1) seluruh fase tektonik yang memiliki nilai tren N32°E dan N210°E (NE-SW). Alterasi hidrotermal pada sistem urat Banyuresmi terbagi kedalam tiga zona yaitu propilitik (chl-sm±ser±cb), argilik (il±kao), dan silisifikasi (qz). Mineralisasi daerah penelitian didominasi oleh mineral bijih seperti galena, sfalerit, pirit, kalkopirit, digenit, kovelit, bornit hematit, dan pirhotit. Mineral bijih tersebut dijumpai pada urat kuarsa dan kuarsa-lempung yang terdiri dari berbagai macam tekstur mencakup crustiform-colloform, masif, comb, zoning, dogteeth, cockade, dll. Urat-urat tersebut diperkirakan memiliki* comb, zoning, dogteeth, cockade, etc. The veins are estimated to have varying orientations, including NW-SE, E-W, and NE-SW. Based on the characteristics of this study, the Banyuresmi ore vein system shows a propensity to be a low sulfidation epithermal system deposit type.

**Keywords:** Ore-bearing vein, low sulfidation epithermal, hydrothermal alteration, Banyuresmi, West Java

*orientasi yang bervariasi, yaitu NW-SE, E-W, dan NE-SW. Berdasarkan karakteristik pada penelitian ini, sistem urat bijih Banyuresmi menunjukkan adanya kecenderungan sebagai tipe endapan sistem epitermal sulfidasi rendah.*

***Kata Kunci**: Urat pembawa bijih, epitermal sulfidasi rendah, alterasi hidrotermal, Banyuresmi, Jawa Barat*

## INTRODUCTION

The Banyuresmi area is a traditional-scale gold mining, located ±13.6 km in the northern part of the Gunung Pongkor gold deposit, or ±45 km away from Jakarta (Figure 1). Administratively, this area is the Cigudeg District, Bogor Regency, West Java Province. In 2017, in the northern part of the study area, a geochemical study was conducted using the soil sampling method, which showed the results of the anomalous distribution of several elements, namely Au, Ag, Cu, Pb, and Zn. Based on this study, it is known that the prospecting zone with high concentrations of Au and Ag elements is in volcanic breccia rocks (Noor & Rachmanto, 2017).

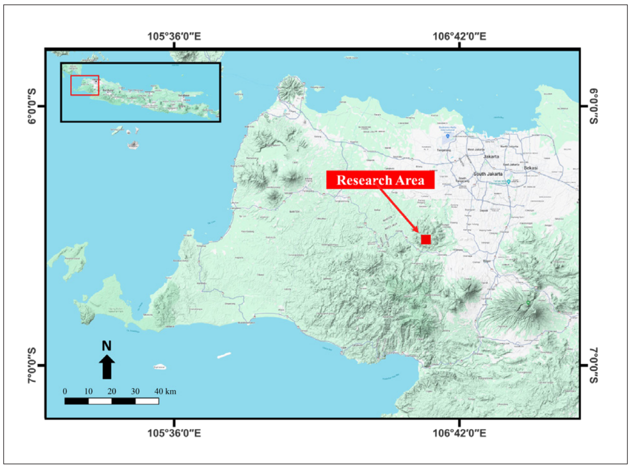


Figure 1. Area of study

Furthermore, it is also known that the ore-bearing veins system is being operated by small-scale and traditional gold mines. Up to now, no peer-reviewed papers have been published on the geological conditions and ore characteristics in this area. Therefore, this study aims to determine the distribution of lithology, geological structure, alteration zonation, and the mineralization characteristics of ore-bearing veins in the Banyuresmi area.

## REGIONAL GEOLOGY

The Banyuresmi area is in the Bogor Geological Map Sheet 1:100,000 Scale (Effendi *et al.*, 1998). The regional rock units in the area of study and its surroundings are Undifferentiated Volcanic Rocks (Qvu) and Volcanic Breccias (Qvb) (Figure 4). Undifferentiated Volcanic Rock (Qvu) consists of breccia and andesitic lava flows. This unit is estimated to be Pleistocene in age. Meanwhile, volcanic breccia (Qvb) consists of andesite-basalt breccia and locally weathered agglomerate. This unit is also Pleistocene in age (Effendi *et al.*, 1998). According to Martodjojo (1984), the geological structures that develop around the area of study include lineaments trending north-south (N-S) and folds trending relatively west-east (E-W) (Figure 2).

The Banyuresmi area is the edge of the Bayah Dome. Mineralization that commonly occurs in this physiography is low sulfidation epithermal. This is characterized by the presence of veins with a crustiform-colloform texture (Prihatmoko & Idrus, 2020) (Figure 3).

The elemental anomaly pattern of the Banyuresmi Prospect, based on soil sampling, showed high gold (Au) and silver (Ag) values. The highest gold anomaly detected at more than 100 ppb (Noor & Rachmanto, 2017).


Figure 2. Geological Structure Map of Western Java based on field, seismic, and gravimetric data. The red box shows the area of study (From Martodjojo, 1984)

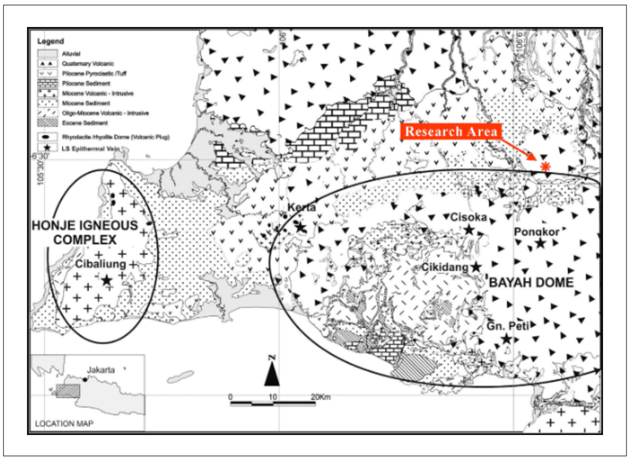


Figure 3. Low sulfidation epithermal prospect map in West Java. The red symbol shows the area of study (From Prihatmoko & Idrus, 2020).

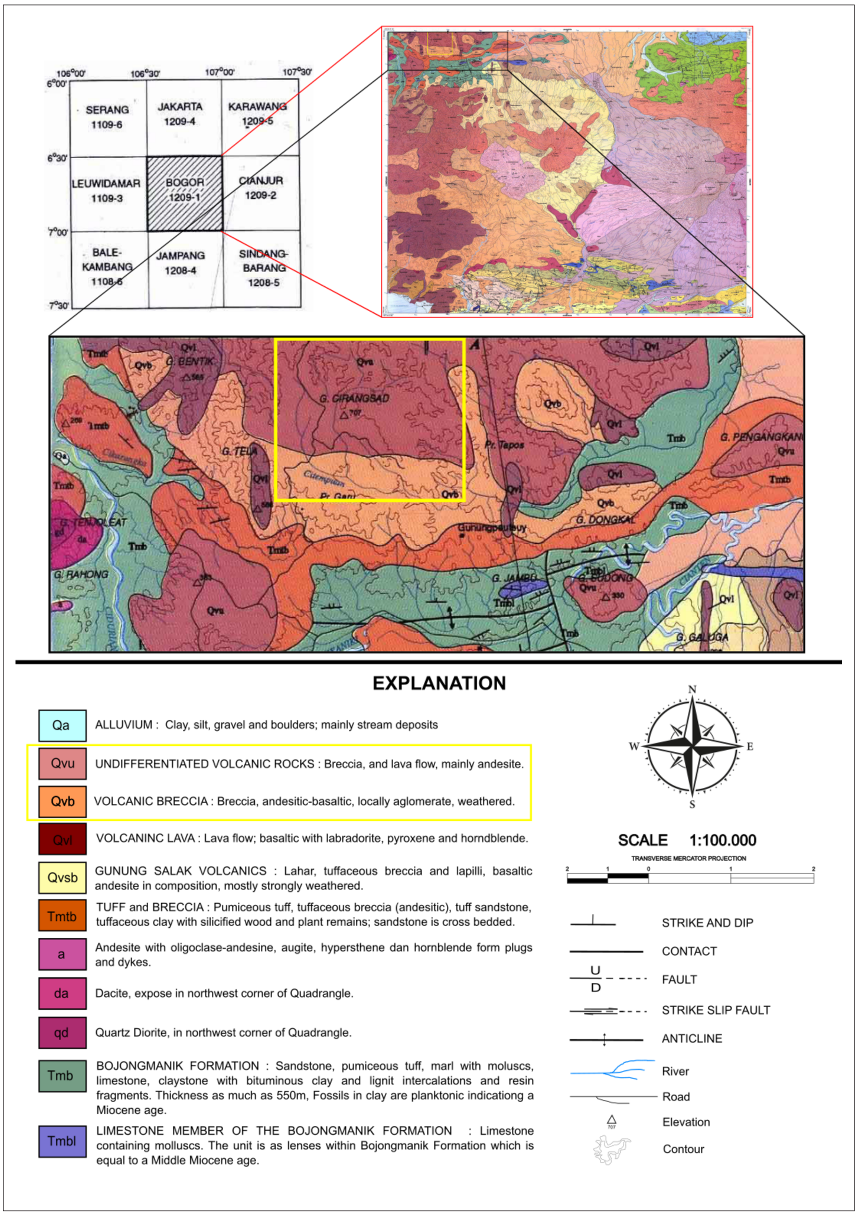


Figure 4. Regional geological map of Bogor sheet (Effendi *et al.*, 1998). The yellow box (  ) is the area of study

## DATA AND METHODOLOGY

This study was conducted using a literature study, fieldwork, stereographic analysis, and laboratory analysis. Observations were conducted over an area of 16 km2 (4x4 km) with a scale of 1:20,000. Fieldwork includes collecting geological data in lithology, geological structure, hydrothermal alteration, and mineralization.

The stereographic analysis was carried out to project data with a three-dimensional orientation into a two-dimensional plane using a stereonet, which allowed the visualization and analysis of the spatial relationships, deformation patterns, and stress distributions within geological structures (Fossen, 2010). Geological structure data obtained in the field consists of shear fractures, gash fractures, fault planes, veins, and veinlets (Figure 9). Meanwhile, laboratory work was focused on the study of 6 rock samples for petrography and 6 vein samples for ore microscopy, which were conducted at the Universitas Pertamina microscope laboratory.

## RESULTS

### Lithology

Based on the results of fieldwork, the lithology in the Banyuresmi area can be devided into at least three rock units (Figure 8) as described below:

### Porphyritic Andesite Unit

This unit is characterized by a light gray, greenish to dark gray color, the primary structure is massive with local sheeting joints, porphyritic texture, euhedral to subhedral crystal form, inequigranular inter-crystal relationships, plagioclase phenocrysts measuring 2-3 mm, and groundmass <2 mm composed of glass material. Outcrops in this unit show slight to moderate weathering conditions (Figure 5). This unit is equivalent to andesite from Pleistocene Inseparable Volcanic Rocks (Qvu) (Effendi et al., 1998).


Figure 5. Outcrop of porphyritic andesite units in the area of study

### Lapilli Tuff Unit

This unit has the characteristics of a grayish-white to reddish-gray color, massive texture, k-feldspar is angular to subrounded, the relationship between clasts is matrix-supported, the clasts measuring 2-5 mm consist of quartz, and the matrix, <2 mm composed of ash-sized volcanic material. Outcrops of lapilli tuff units show slight to total weathering conditions (Figure 6). This unit is interpreted as equivalent to the Pleistocene Undifferentiated Volcanic Rock (Qvu) (Effendi *et al.*, 1998).


Figure 6. Outcrop of lapilli tuff units in the area of study.

## Colluvial Unit

This unit is characterized by unconsolidated rocks, ranging from gravel to boulders (4 to >256 mm), consisting of chunks of andesite rock with a porphyritic texture, euhedral to subhedral crystals, inequigranular, phenocrysts consisting of plagioclase, clinopyroxene, and xenoliths, measuring 2-3 mm, and the matrix measuring <2 mm is a clay mineral. This unit is interpreted as the result of the fragmentation of Volcanic Breccia (Qvb) on the Bogor Geological Map Sheet (Effendi *et al.*, 1998) (Figure 7).


Figure 7. Overlay of the Colluvial Unit in the south of the study area

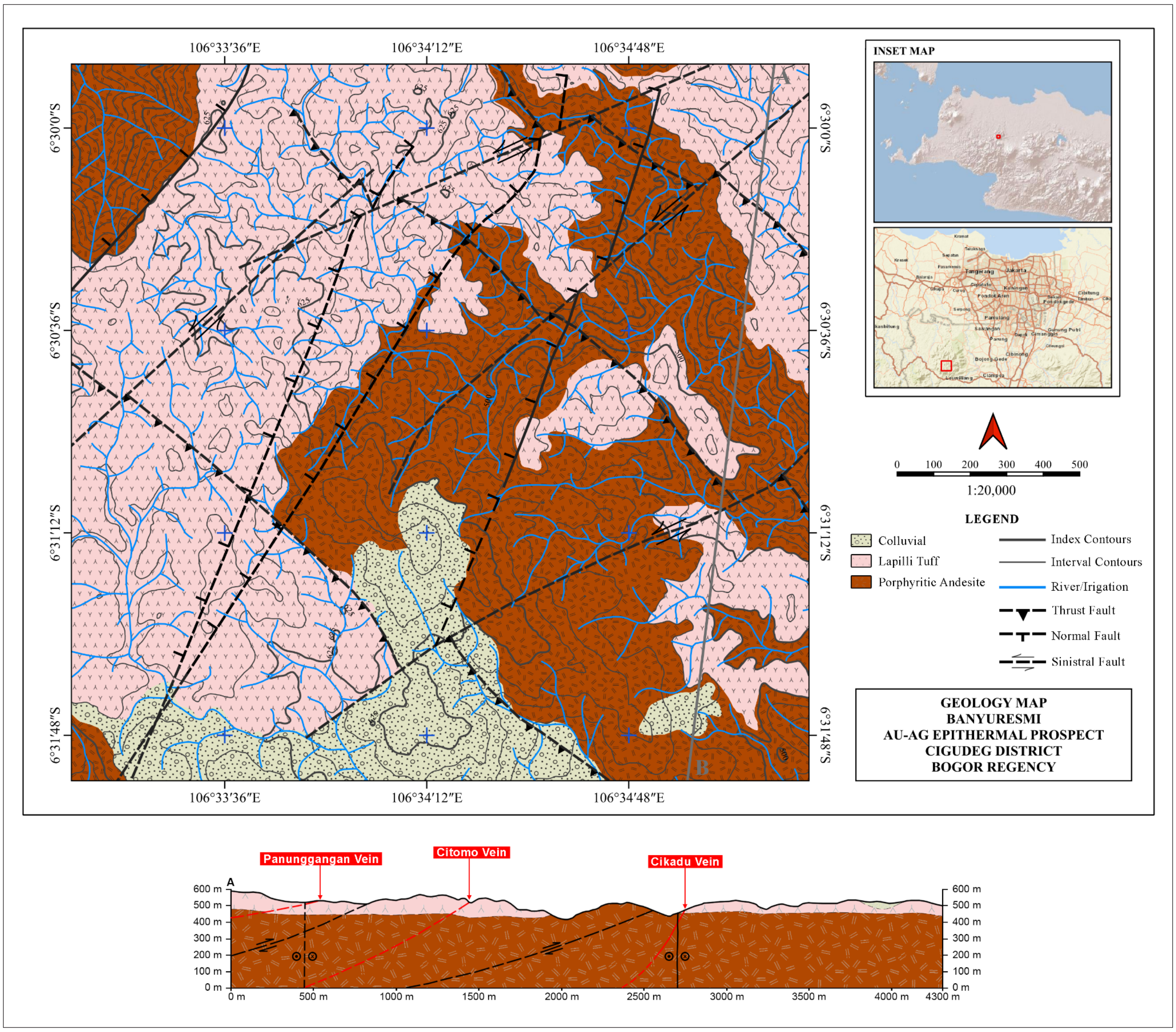


Figure 8. Geological map and cross-section of Banyuresmi and surrounding areas

## GEOLOGICAL STRUCTURES

Structural geology of the study area, can be divided into at least six structural subdivisions based on its structural infill and the cross-cutting relationship in the stratigraphy approach (Figure 9). The six structural subdivisions in the Banyuresmi area are divided into shear joints on porphyritic andesite, extension joints on porphyritic andesite, shear joints on lapilli tuff, extension joints on lapilli tuff, shear vein, and extension vein on both rocks.

In dynamic analysis, σ1 is the maximum stress, which is interpreted as the direction of the main stress, σ2 is the intermediate stress, which is the trend of the structural plane, and σ3 is the minimum stress, which is the direction of the structural plane opening.

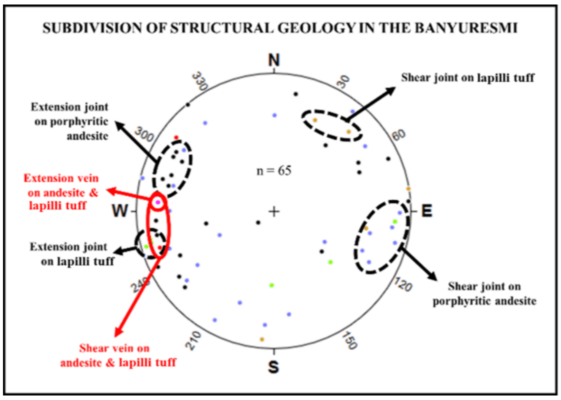


Figure 9. Subdivision of geological structure data in the Banyuresmi area

The first deformation stage ($D_1$) is characterized by the presence of shear joints and extension joints in porphyritic andesite units. Shear joints have general values of N201°E/63° and N187°E/81°. The tectonic forces that deform porphyritic andesite at this stage are interpreted as having a maximum stress (σ1): 63°, N61°E, intermediate stress (σ2): 17°, N190°E, and minimum stress (σ3): 19°, N286°E (Figure 10).

The second deformation stage ($D_2$) is characterized by the presence of shear and extension joints in lapilli tuff units. The results of the dynamic analysis show the general value of the shear joint. The tectonic deformation force in this second stage has a maximum stress value (σ1): 18°, N349°E, intermediate stress (σ2): 70°, N150°E, and a minimum stress (σ3): 7, N257°E (Figure 11).

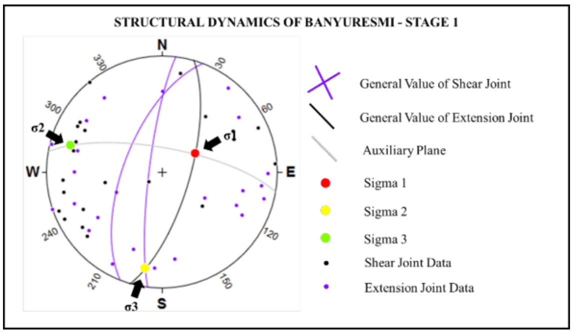


Figure 10. Dynamic model of the first deformation stage ($D_1$) in the Banyuresmi area

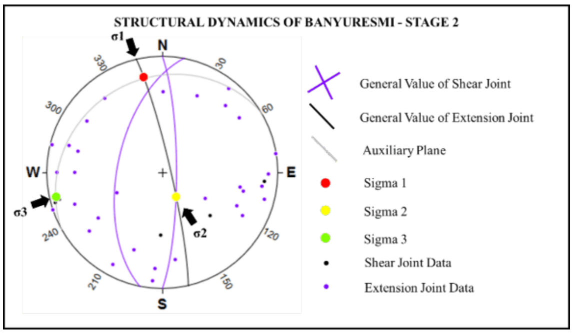


Figure 11. Dynamic model of the second deformation stage ($D_2$) in the Banyuresmi area

The third deformation stage ($D_3$) is interpreted as the deformation stage that brought mineralization. Ore vein mineralization occurs in both rock units. Shear veins have a general value of N342°E/75° and N37°E/77°, while extension veins are priced at N4°E/73°. The dynamic model at this stage shows the main stress (σ1): 11, N215°E, intermediate stress (σ2): 73°, N84°E, and minimum stress (σ3): 11°, N307°E (Figure 12).

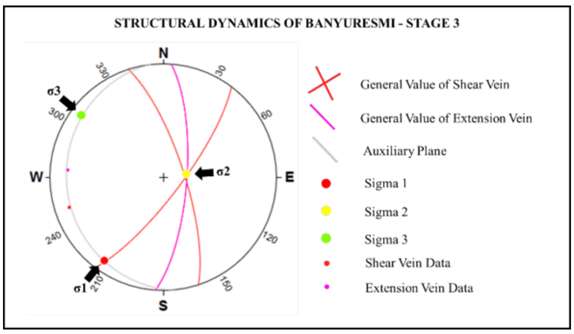


Figure 12. Dynamic model of the third deformation stage ($D_3$) in the Banyuresmi area

The model of the geological structure in the area of study is generated from the average maximum stress value (σ1) of all deformation stages ($D_1$, $D_2$, and $D_3$) to make it a more general dynamics model. This model has trend values of N32°E and N210°E (NE-SW) and correlated with the interpretation of straightness (Figure 13).

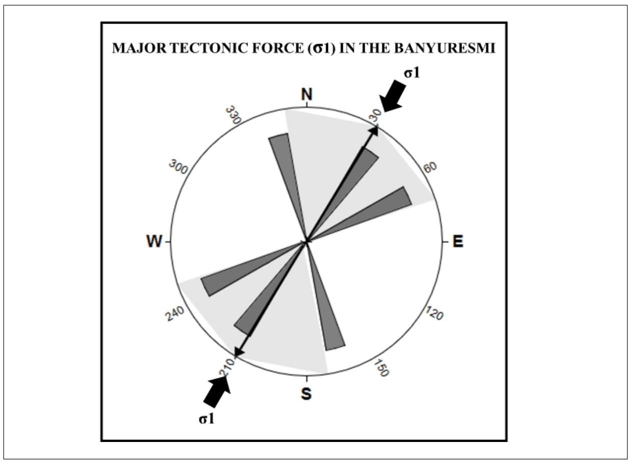


Figure 13. General model of geological structure dynamics in the Banyuresmi ore-bearing vein system

Based on fault direction patterns, the West Java and Banten regions have 4 structural patterns, respectively the Meratus Pattern (NE-SW), the Sunda Pattern (N-S), the Sumatra Pattern (NW-SE), and the Java Pattern (E-W). (Marotodjojo, 1984; Helmi & Haryanto, 2008). The dynamics analysis described previously shows that the first tectonic stage ($D_1$) produced a dominant NE-SW structural pattern similar to the Meratus Pattern. In the second tectonic stage ($D_2$), it has a dominant NW-SE structural pattern, which has the same pattern as the Sumatran Pattern. Meanwhile, the third tectonic stage ($D_3$) produced a dominant NE-SW structural pattern, the same as the Meratus Pattern. The structural pattern in the third tectonic stage ($D_3$) has a pattern that tends to be the same as the first stage ($D_1$), which is thought to occur due to a delusion of stress direction caused by local tectonic activity or influenced by small faults from large fault activity on the western part of Java Island.

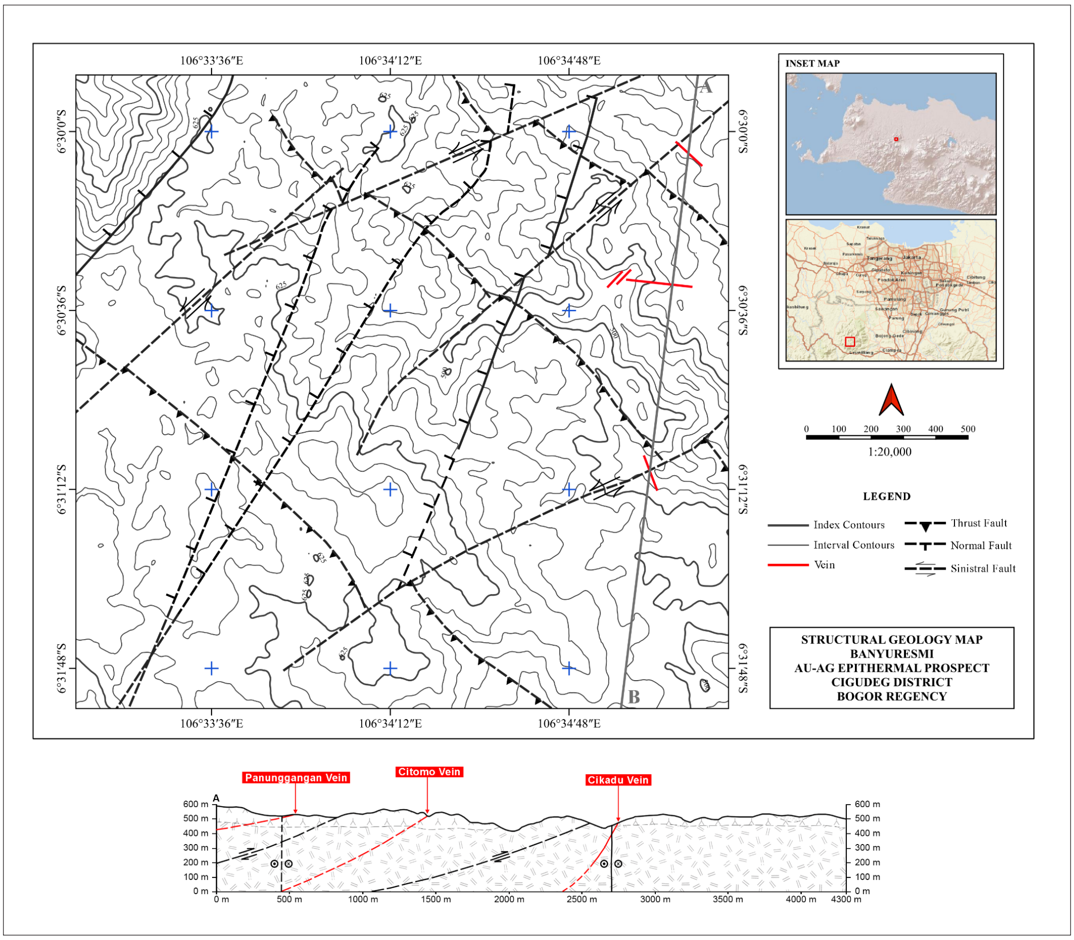


Figure 14. Geological structure map and cross-section of Banyuresmi and surrounding areas

## HYDROTHERMAL ALTERATION

Based on fieldwork, macroscopic descriptions, and microscopic descriptions, there are three types of alteration in the area of study, which consist of propylitic, argillic, and silicification (Figure 19). In detail, the zones can be explained as follows:

### Propylitic (Chlorite-Smectite±Sericite ±Carbonate)

The propylitic zone makes up 8.75% of the total study area and is spread across the central to eastern parts of the study area. This alteration is found in porphyritic andesite units with moderate to intense alteration intensity (Figure 15).


Figure 15. Outcrop of intense propylitic alteration of porphyritic andesite

Macroscopic observations of propylitic alteration show greenish-gray rocks. The greenish color of this alteration tends to be influenced by the presence of chlorite and chlorite-smectite minerals. The presence of carbonate minerals is indicated by the mineral's reaction to HCl liquid. Oxide minerals are marked by the presence of yellowish-brown minerals. Meanwhile, from petrographic analysis, secondary minerals were found, such as secondary quartz, clay minerals, calcite, chlorite, and opaque minerals (Figure 18A-D). This zone is interpreted to be formed around 200-310°C (Hedenquist *et al.*, 1996).

### ARGILLIC (ILLITE±KAOLINITE)

The argillic zone covers 33.7% of the study area and extends from the west to the east. This alteration zone is found in tuff and porphyritic andesite units with moderate to strong alteration intensity (Figure 16).

Macroscopic observations of argillic alteration in the field show grayish-white to yellowish-brown rocks. The presence of clay minerals is indicated by white clay-sized minerals, while the presence of yellowish-brown minerals indicates oxide minerals. Meanwhile, from petrographic analysis, secondary minerals such as secondary quartz, clay minerals, iron oxide, and opaque minerals were found (Figure 18E-H). This zone is interpreted to have formed at 100-210°C (Hedenquist *et al.*, 1996).


Figure 16. Outcrop of strong argillic alteration of lapilli tuff

### Silicification (Quartz)

The silicification zone constitutes approximately 0.86% of the area studied in total. This zone is local to the study area and generally alters lapilli tuff units with moderate to intense intensity (Figure 17).

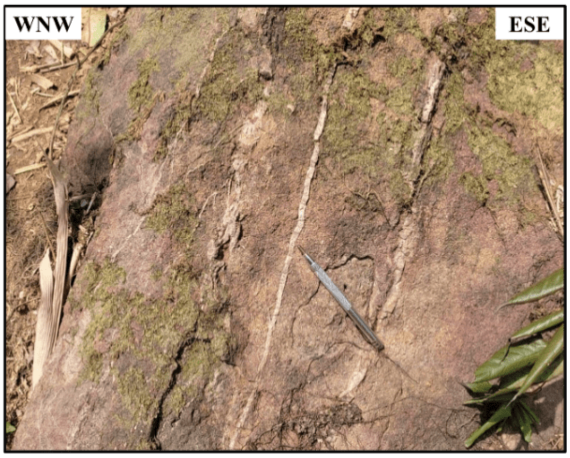


Figure 17. Outcrop of strong silicification alteration of lapilli tuff

Macroscopic observations of silicification alteration in the field show brownish-gray rocks. The presence of silica minerals and secondary quartz around the quartz veinlets characterizes this alteration. This zone is interpreted as formed at 200-330°C (Hedenquist *et al.*, 1996).

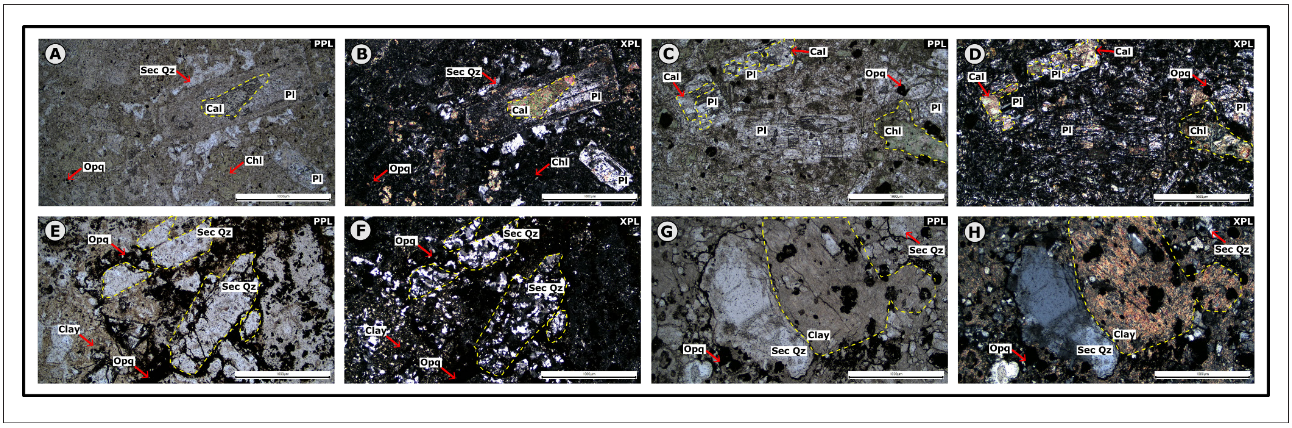


Figure 18. Photomicrographs of the different alteration styles at Cigudeg. (A-B) Propylitic alteration in porphyritic andesitic with plagioclase which replaced with calcite, groundmass altered to chlorite and secondary quartz; (C-D) Plagioclase replaced with calcite and an alteration of chlorite after mafic minerals, disseminated opaque minerals (probably pyrite) ; (E-F) Plagioclase altered to secondary quartz, matrix replaced mostly by clay minerals, opaque minerals strongly oxidized matrix (probably hematite); (G-H). Secondary quartz and clay replacement on both plagioclase and matrix in lapilli tuff, disseminated opaque minerals (probably pyrite). Sec Qz = secondary quartz; Opq = opaque minerals; Cal = calcite; Pl = plagioclase; Clay = clay minerals; Chl = chlorite

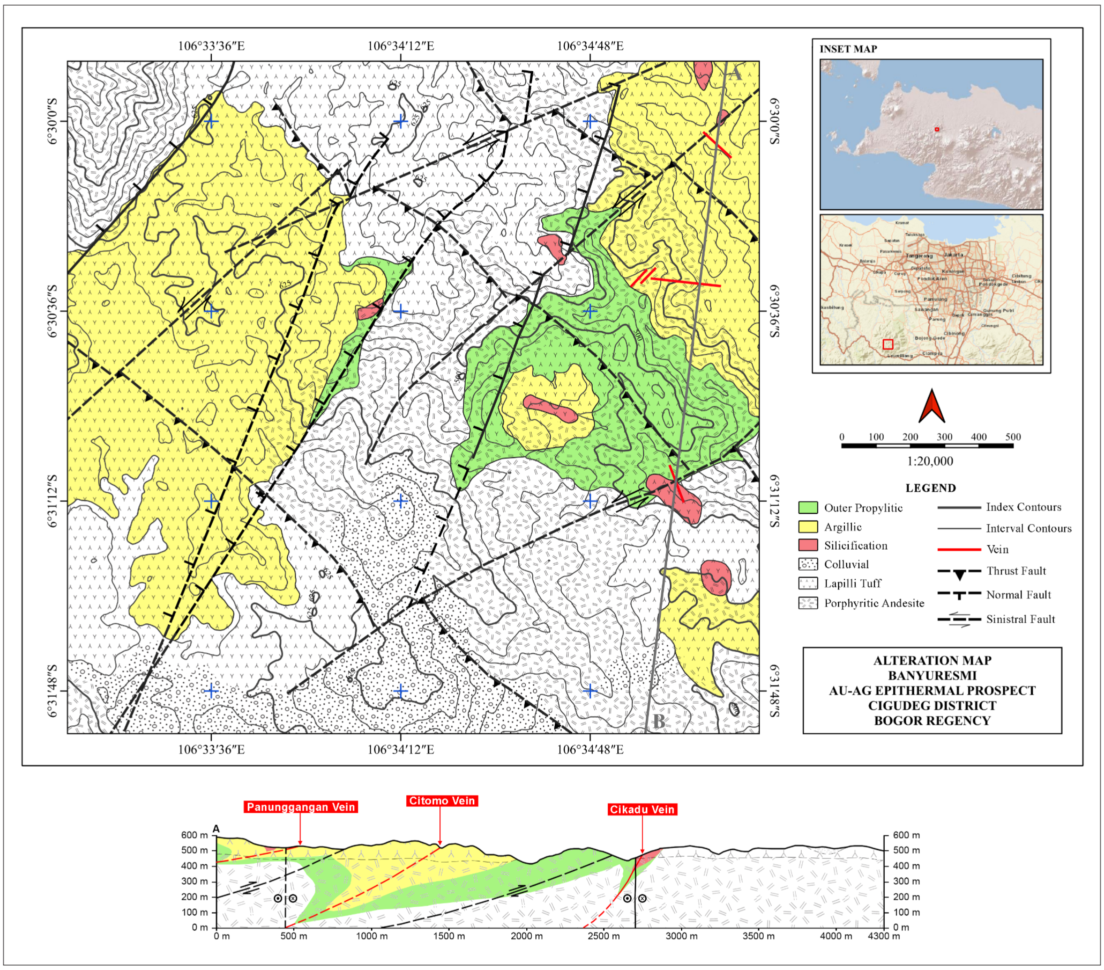


Figure 19. Hydrothermal alteration map and cross-section of the Banyuresmi and surroundings area

## ORE MINERALIZATION

The main veins discovered in the area of study consist of Lembah Panunggangan, Lembah Pasir Heas, Lembah Citomo, Lembah Cilangkap, and Bukit Cikadu. Below is a detailed description of the mineralization domains.

### Lembah Panunggangan (Quartz± Rhodonite)

Macroscopically, the Lembah Panunggangan mineralization has a northwest-southeast (NW-SE) orientation with crustiform-colloform, drusy, comb, and zoning vein textures (Figure 28A). The gangue mineral observed in this vein is quartz ± rhodonite. Meanwhile, the ore minerals formed in this vein are disseminated pyrite ($FeS_2$), and oxide minerals are also present in this vein, including hematite-goethite-jarosite and dendritic manganese oxide. Microscopically, mineralization in the Lembah Panunggangan consists of galena (PbS) that is surrounded by hematite ($Fe_2O_3$), characterized by the red internal reflection (Figure 20).

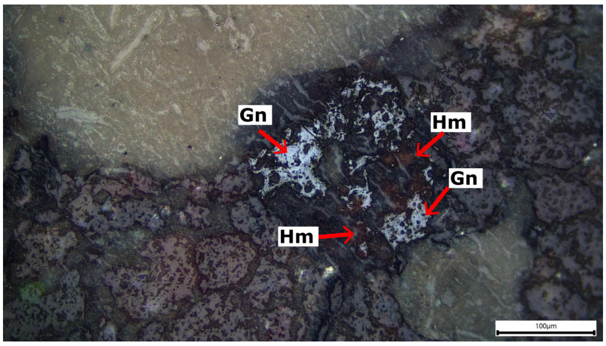


Figure 20. The polished section image from the Lembah Panunggangan vein showing the presence of galena (Gn) and sphalerite (Sph)

### Lembah Pasir Heas (Quartz±Albite)

Macroscopically, the Lembah Pasir Heas mineralization has an ore mineral composition of disseminated pyrite ($FeS_2$) and galena (PbS). Meanwhile, quartz ± albite is present as a gangue mineral. The vein textures found in this vein include crustiform, massive, comb, and dog teeth (Figure 28B). The Pasir Heas Vein was also found in an oxidized condition characterized by the presence of hematite-jarosite.

Mineragraphic observations show that the ore minerals formed in this vein include cubic pyrite ($FeS_2$) overgrown by anhedral digenite ($Cu_9S$) (Figure 21). Sphalerite (ZnS) is surrounded by larger cubic grains of pyrite ($FeS_2$) and minor pyrrhotite ($Fe_7S_8$) (Figure 22).

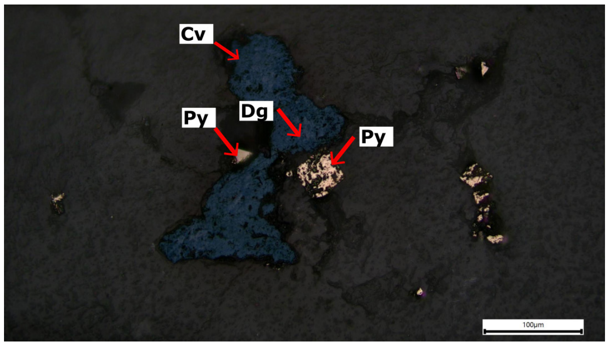


Figure 21. A polished section image from the Lembah Pasir Heas vein showing the presence of pyrite (Py), covellite (Cv), and digenite (Dg)

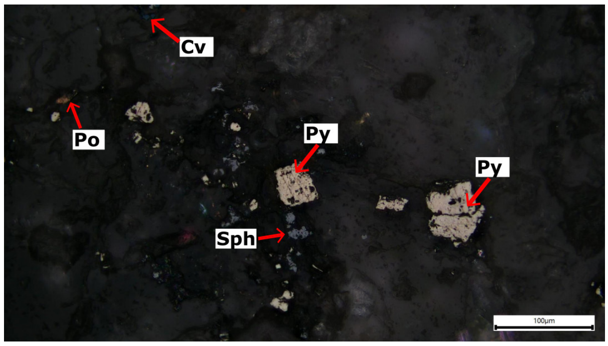


Figure 22. The polished section image from the Lembah Pasir Heas vein shows the presence of pyrite (Py), sphalerite (Sph), covellite (Cv), and pyrrhotite (Po)

### Lembah Citomo (Quartz±Alunite)

Lembah Citomo mineralization is estimated to have an east-west (E-W) and northeast-southwest (NE-SW) orientation. The textures found in this vein include a comb, crustiform, sugary, massive, and crystalline, with a composition of quartz ± alunite. Hematite is also present as an oxidation product of the vein (Figure 28C).

Based on mineragraphic observations, the ore minerals formed in the Lembah Citomo is a large mass of galena (PbS) with an exsolution intergrowth of tiny chalcopyrite ($CuFeS_2$) grains (Figure 23). There is also a fracture filling of bornite ($Cu_5FeS_4$) and chalcopyrite ($CuFeS_2$) grains (pseudomorph after pyrite), replaced by digenite ($Cu_9S$), covellite (CuS), and minor malachite ($Cu_2CO_3(OH)_2$), surrounded by anhedral pyrite ($FeS_2$) (Figure 24).

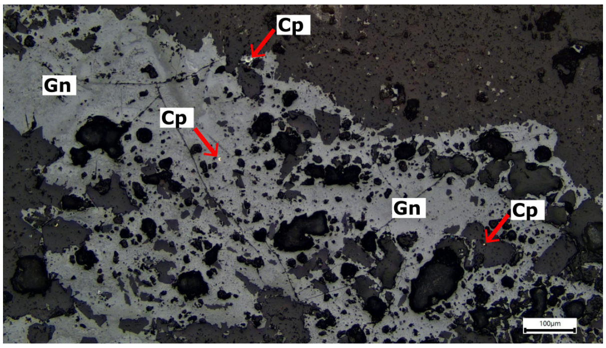


Figure 23. The polished section image from the Lembah Citomo vein shows the presence of galena (Gn) and chalcopyrite (Cp)

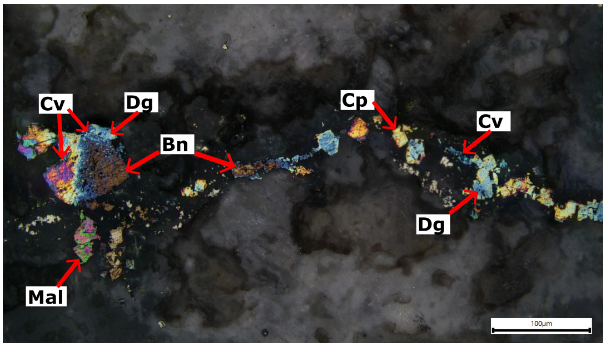


Figure 24. A polished section image from the Lembah Citomo vein showing the presence of bornite (Bn), chalcopyrite (Cp), digenite (Dg), covellite (Cv), and malachite (Mal)

## Lembah Cilangkap (Quartz-Clay±Alunite)

Mineralization in this area, macroscopically, has an ore mineral composition of disseminated pyrite ($FeS_2$) and quartz-clay ± alunite gangue minerals. The textures found in these veins include massive, cockade, and patchy. Manganese oxide (MnO) present as an oxidation product of the vein (Figure 28E).

Mineragraphic observations show that the ore minerals formed in this vein include galena (PbS), which is surrounded by thin tabular hematite ($Fe_2O_3$), overgrown by chalcopyrite ($CuFeS_2$) with some replacement of bornite ($Cu_5FeS_4$) (Figure 25). There is also bornite ($CuFeS_2$) and covellite (CuS) replacing a thin tabular hematite ($Fe_2O_3$) (Figure 26).

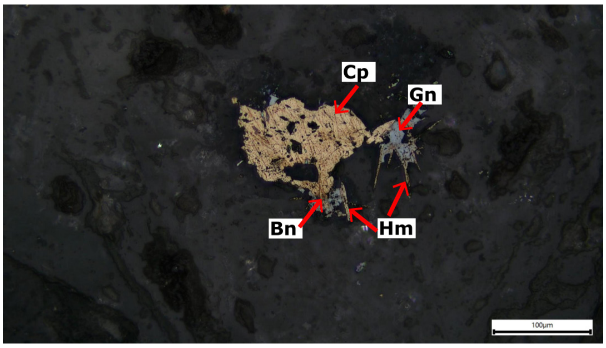


Figure 25. A polished section image from the Lembah Cilangkap vein showing the presence of chalcopyrite (Cp), galena (Gn), bornite (Bn), and hematite (Hm)

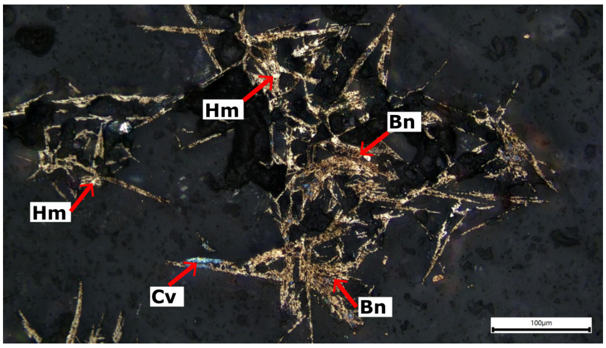


Figure 26. The polished section image from the Lembah Cilangkap vein showing the presence of hematite (Hm), bornite (Bn), and covellite (Cv)

## Bukit Cikadu

The Bukit Cikadu mineralization (Figure 27) has a vuggy-bladed texture with a composition of quartz, oxide minerals, and sulfide minerals (sphalerite?) (Figure 28F). The veins in Bukit Cikadu were formed in lapilli tuff units with strong silicification and clay alteration.

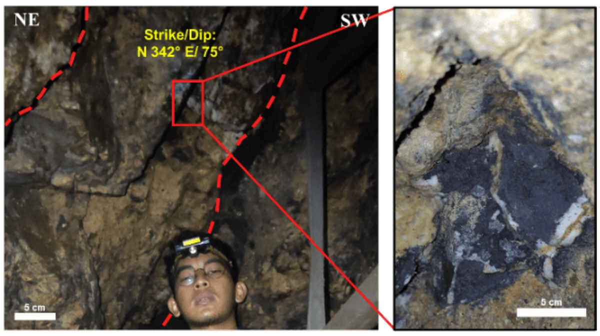


Figure 27. Appearance of Bukit Cikadu vein

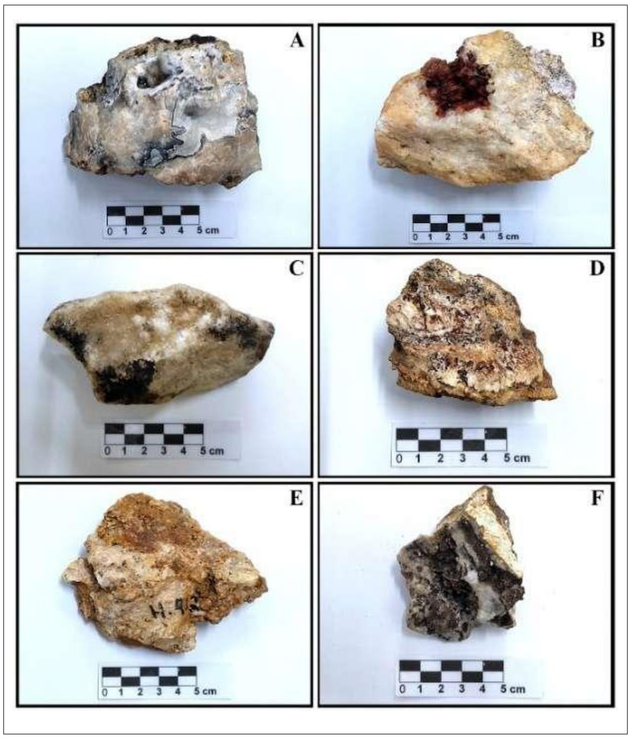


Figure 28. Representative vein specimens in the area of study

## Ore Paragenesis

Based on ore microscopy analysis, by observing the temperature of their formations and the genesis texture, there have been two stages that occurred in the area of study. The stages are divided into the hydrothermal stages and the supergene stage.

In the hydrothermal stage, pyrite forms across a broad temperature range of 350–100°C, spanning both high and low sulfidation systems. Chalcopyrite typically crystallizes at 350–200°C, aligning with intermediate-sulfidation conditions, while pyrrhotite develops under lower sulfidation states within 350–200°C. Bornite is stable at 350–250°C, occurring in intermediate-sulfidation zones, similar to hematite, which forms in oxidized high-sulfidation environments or certain low sulfidation settings, at 350–250°C. Galena and sphalerite crystallize over a broader range; galena forms within 300–100°C, generally in intermediate to low sulfidation settings, while sphalerite spans 350–100°C, adjusting to varying sulfidation conditions (Einaudi *et al*., 2003; Putz *et al*., 2009; Neumann, 2020). Meanwhile, in the supergene stage, hematite forms at <100°C through oxidation of iron-bearing minerals, digenite forms at 200–100°C as a secondary copper sulfide, covellite develops at 150–50°C through oxidation and enrichment processes, while malachite precipitates at <50°C, typically in near-surface oxidized environments (Einaudi *et al*., 2003; Putz *et al*., 2009; Neumann, 2020).

Table 1. Paragenesis of ore minerals in the Banyuresmi ore-bearing vein (a range taken from Eunaudi *et al.*, 2003; Putz *et al.*, 2009; Neumann, 2020)

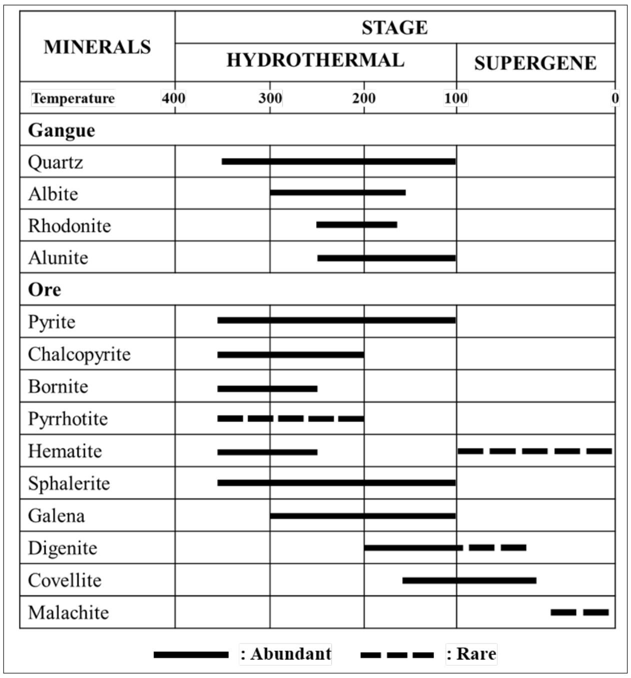


## DISCUSSION

The widest distribution of hydrothermal alteration products and ore mineralization is generally found in lapilli tuff lithology. This is closely related to the high porosity and permeability properties of the lapilli tuff, which are very favourable for hydrothermal fluid flow. The porosity of a pyroclastic rock generally imparts a primary permeability. This permeability may change as a result of the dissolution of glass and the growth of secondary minerals (Kenneth and Heiken, 1992). This permeability is also associated with the geological structure as the main pathway for hydrothermal fluid flow.

The geological structure of the andesite unit is interpreted as a relative dynamic value. Meanwhile, the geological structure that deforms the lapilli tuff unit is interpreted as the absolute maximum stress (σ1). This is because there is a possibility that the andesite unit was also deformed when the lapilli tuff unit was deposited at a younger age.

By analyzing the kinematics of the vein planes, under the influence of stress and strain, the responses to dynamic forces and the conditions under which mineralization occurs can be determined (Davis & Reynolds, 1996). Based on these, the kinematics of the vein plane will follow the dynamic model (major force) acting on that plane. It is interpreted that mineralization occurs when maximum stress has a value of 11, N215°E.

The types of faults produced in this area of study are interpreted based on the direction of maximum stress. Generally, thrust faults have a relationship perpendicular to the direction of the main stress (σ1). In a thrust fault regime, the maximum compressive stress (σ1) is horizontal, and the thrust faults form perpendicular to this direction (Anderson, 1960). The strike-slip faults in the area of study are parallel to the main stress. Meanwhile, normal faults have a relationship that is relatively perpendicular to the main stress but is 15° larger or smaller than the angle of the main stress.

Based on structural dynamics in the Banyuresmi, the Bukit Cikadu vein is interpreted as a compressional regime during the first ($D_1$) or second deformation stage ($D_2$). This regime makes this vein have three possible vein models that may form, namely thrust vein, which has relatively steep dipping with dilational jog inflation of width at some point along the plane, or a compressional bedding vein, which has relatively gentle dipping (Corbett, 2013).

Alternatively, based on geometry analysis, the Bukit Cikadu vein shows the structural signature. This vein is more likely an extensional underlapping/overlapping product that has constant width when increasing depth, The vein geometry observed in the Bukit Cikadu is estimated to have a constant width of 30 cm with a constant planar shape below the surface which generally has a perpendicular relationship to the main stress and has a relatively upright dipping value (75°) (Figure 22). Based on this explanation, it is interpreted that the Bukit Cikadu vein is strongly the product of structures that are produced by extensional underlapping/overlapping zones, which are potential assemblage zones of two strike-slip faults that are generated by NE-SW maximum stress (Micklethwaite *et al.*, 2010).

The presence of heterogeneous vein texture in the area of study also indicates a hydrothermal process. The cockade and patchy texture that is found in the Cilangkap vein has been interpreted as undergoing repeated injections of hydrothermal fluid. This is because both texture shows the quartz and clay from the different fluid stages inside the last mineralized quartz (Frenzel & Woodcock, 2014). On the other side, the bladed texture found in Cikadu has been interpreted as being formed in the boiling zone (Etoh *et al.*, 2002).

The presence of a banded texture reinforced with high Au and Ag anomalous elements indicates that the Banyuresmi area has a low sulfidation epithermal system (Noor & Rachmanto, 2017). This has similarities with the characteristics of low sulfidation epithermal deposits in the Bayah Dome Complex, such as Cisoka, Pongkor, and Cibaliung (Prihatmoko & Idrus, 2020).

## CONCLUSIONS

Based on the studies that have been conducted, it can be concluded that Lapilli tuff lithology, which is permeable and extensive, is the key lithology in the distribution process of alteration and mineralization. The geological structure in the area of study is divided into several subdivisions formed from the deformation stage. The initial deformation stage ($D_1$) is characterized by the presence of shear joints and extension joints in the porphyritic andesite unit. The second deformation stage ($D_2$) is characterized by the presence of shear and extension joints in the lapilli tuff unit. Meanwhile, the third deformation stage ($D_3$) is interpreted as the tectonic stage that brought mineralization. All deformation stages have trend values of N32°E and N210°E (NE-SW).

Ore minerals in the Banyuresmi Prospect can be divided into two types of products, namely hydrothermal and supergene. Hydrothermal products consist of pyrite, digenite, galena, pyrrhotite, chalcopyrite, and sphalerite. Meanwhile, supergene consists of covellite, bornite, malachite, and hematite. The vein trend shows an east-relative northeast-west relative southwest direction (ENE-WSW). Vein textures found on the Banyuresmi Prospect include massive, banded (crustiform-colloform), comb, sugary, drusy, dogteeth, vuggy, bladed, and rimming. The presence of a banded texture and soil anomalies that have high Au-Ag indicates a low sulfidation epithermal type deposit.

Recommendations for further studies in the Banyuresmi area are to conduct fluid inclusion study to confirm the deposit type through temperature and salinity based on the Wilkinson (2001) diagram.

**ACKNOWLEDGEMENTS**

On this occasion, the authors would like to thank the Lecturers of the Geological Engineering Department at Universitas Pertamina for the guidance and knowledge provided during the lecture. Likewise, the authors also express their gratitude for the second-year establishment of the Masyarakat Geologi Ekonomi Indonesia Student Chapter Universitas Pertamina (MGEI-SC Universitas Pertamina), which coincided with the completion of this scientific work.

**REFERENCES**

Anderson, E. M. 1951. *The Dynamics of Faulting and Dyke Formation with Applications to Britain. Second Edition.* Edinburgh: Oliver & Boyd Ltd.

Bernhard, J.K., Barnett, W., Uken, R., and Myers, R. 2020. Structural Analysis of Drill Core for Mineral Exploration and Mining Review and Workflow Toward Domain-Based-3D Interpretation. *Reviews in Economic Geology Vol 21*, pp.215-245. Colorado: Society of Economic Geologists. DOI: 10.5382/rev.21.07

Castroviejo, R. 2023 *A Practical Guide to Ore Microscopy - Volume 1*. Switzerland: Springer Cham. DOI: 10.1007/978-3-031-12654-3_43

Corbett, G., and Leach, T. 1997. *Southwest Pacific Rim Gold-Copper Systems: Structure, Alteration, and Mineralization Short Course Manual*. New Zealand: CMS New Zealand Ltd.

Corbett, G. 2013. Pacific Rim Epithermal Au-Ag. Proceedings, *World Gold Conference, AAusIMM Publication No.9*, pp.5-13. Brisbane: Australasian Institute of Mining and Metallurgy. DOI:10.13140/2.1.2691.3286

Craig, J. R., and Vaughan, D. J. 1994. *Ore Microscopy and Ore Petrography*. John Wiley & Sons.

Davis, G. H., and Reynolds, S. J. 1996. *Structural Geology of Rocks and Regions*. New Jersey: John Wiley & Sons.

Effendi, A.C., Kusnama, K., and Hermanto, B. 1998. *Geological Map Sheet of Bogor, Java. Second Edition*. Bandung: Center for Geological Research and Development

Eunaudi, M.T., Hedenquist, J.W., and Inan, E.E. 2003. Sulfidation State of Fluids in Active and Extinct Hydrothermal Systems: Transitions from Porphyry to Epithermal Environment. *Society of Economic Geologists Special Publication 10, Vol. Giggenbach*. Colorado: Society of Economic Geologists

Etoh, J., Izawa, E., Watanabe, K., Taguchi, S., and Sekine R. 2002. Bladed Quartz and Its Relationship to Gold Mineralization in the Hishikari Low-Sulfidation Epithermal Gold Deposit, Japan. *Economic Geology Vol 97(8)*, pp.1841–1851. DOI: 10.2113/gsecongeo.97.8.1841

Fossen, H. 2010. *Structural Geology*. Cambridge University Press, Cambridge, 463. DOI: 10.1017/CBO9780511777806

Frenzel, M., and Woodcock, N. 2014. Cockade Breccia: Product of Mineralisation Along Dilational Faults. *Journal of Structural Geology Vol 68*. DOI: 10.1016/j.jsg.2014.09.001.

Hedenquist, J. W., Izawa, E., Arribas, A. and White, N. C. 1996. Epithermal Gold Deposits: Styles, Characteristics and Exploration. No. 1. Resources Geology Special Publication.

Helmi, F. and Haryanto, I. 2008. Pola Struktur Regional Jawa Barat. *Bulletin of Scientific Contribution, 6(1)*, pp.57-66.

Ineson, P.R. 1989. *Introduction to Practical Ore Microscopy. 1st edition*. London: Routledge. DOI: 10.4324/9781315841205

Zhao, J., Brugger, J., Ngothai, Y., and Pring, A. 2014. The Replacement of Chalcopyrite by Bornite Under Hydrothermal Conditions. *American Mineralogist* Vol 99(11-12): 2389–2397. DOI: 10.2138/am-2014-4825

Perkins, D., and Henley, R. W. 2020. Hydrothermal ore deposits. In book: *Mineralogy - An Introduction to the Study of Minerals and Crystals* (pp. 123-135)

Prihatmoko, S., and Idrus, A. 2020. Low-sulfidation Epithermal Gold Deposits in Java, Indonesia: Characteristics and Linkage to the Volcano-tectonic Setting. *Ore Geology Reviews Vol 121*. DOI:10.1016/j.oregeorev.2020.103490

Martodjojo, S. 1984. *Evolusi Cekungan Bogor Jawa Barat*. Bandung, pp.1-128. Bandung: Institut Teknologi Bandung.

Micklethwaite, S., Sheldon, H., and Baker, T. 2010. Active Fault and Shear Processes and Their Implications for Mineral Deposit Formation and Discovery. *Journal of Structural Geology - J Structural Geology Vol 32*, pp.151-165. DOI: 10.1016/j.jsg.2009.10.009

Neumann, Udo. 2020. Guide for the Microscopical Identification of Ore and Gangue Minerals (Mineral profiles with photomicrographs) 2nd edition. 10.15496/publikation-38866.

Noor, D., and Rachmanto, H. 2017. *Studi Eksplorasi Geokimia - Metoda Soil Sampling Daerah Margajaya dan Sekitarnya, Kecamatan Cigudeg, Kabupaten Bogor, Jawa Barat*. Bogor: Universitas Pakuan.

Putz, H., Paar, W.H., and Topa, D. 2009. A Contribution to the Knowledge of the Mineralization at Mina Capillitas, Catamarca. *Revista de la Asociación Geológica Argentina Vol.64(3)*, pp. 514 - 524

United States Geological Survey. 2006. *FGDC Digital Cartographic Standard for Geologic Map Symbolization: Pattern Chart*. USGS Doc. No. FGDC-STD-013-2006.

Wilkinson, J.J. 2001. Fluid Inclusions in Hydrothermal Ore Deposits. *Lithos Vol 55*, pp.229–272.

Wohletz, K., and Heiken, G. 1992. *Volcanology and geothermal energy*. University of California Press.